Applying homotopy perturbation method to provide an analytical solution for Newtonian fluid flow on a porous flat plate

Tareq Ghanbari Ashrafi[1], Siamak Hoseinzadeh[2,*], Ali Sohani[3], Mohammad Hassan Shahverdian[3]

[1] Department of Mechanical and Aeronautical Engineering, Islamic Azad University, Bafgh Branch, Yazd, Iran

[2] Department of Mechanical and Aeronautical Engineering, University of Pretoria, Pretoria, South Africa

[3] Lab of Optimization of Thermal Systems' Installations, Faculty of Mechanical Engineering-Energy Division, K. N. Toosi University of Technology, Tehran, Iran

*Correspondence to: S. Hoseinzadeh, Department of Mechanical and Aeronautical Engineering, University of Pretoria, Pretoria, South Africa. Email: hoseinzadeh.siamak@gmail.com; hosseinzadeh.siamak@up.ac.za

Abstract

This research work is going to apply the homotopy perturbation method to solve the problem of flowing Newtonian fluid on a flat plate. For this purpose, initially, the problem, including the governing equations and boundary conditions, is defined, and after that, the considered assumptions to solve the defined problem are introduced. Next, the working principle of the homotopy perturbation method is described, and then, the way to obtain the analytical solution using the homotopy perturbation method is presented, and finally, the accuracy of the proposed analytical solution in comparison to the numerical approach is compared for validation. Both momentum and energy equations are solved. The maple software program is utilized for carrying out the mathematical calculations, while the validation is done using the profiles for stream function, velocity distribution, stress, and dimensionless temperature as the key indicators related to the solution. The conducted comparison shows that the analytical solution provided by the homotopy perturbation method is able to predict all the important performance criteria for the problem very well, and therefore, the homotopy perturbation method has a strong potential to be employed for providing the analytical solution for such problems.

Keywords: analytical solution; flat plate; homotopy perturbation method (HPM); Maple software program; Newtonian fluid; porous media

1 INTRODUCTION

There are many types of porous media in different applications.[1-4] They are extensively employed in fuel cells, cooling of electronic devices, medical science, and so on.[5-8] Having such a variety of applications has motivated several researchers to study them from various viewpoints.[9-12]

In a group of investigations, as the main objective of the research, using porous media to enhance the system performance has been studied.[13-16] For instance, in order to reduce the consumption of energy in a building, Sheikholeslami et al.[17] replaced a smooth channel with the sinusoidal type and also took advantage of porous media and nanoparticles at the same time to improve the heat transfer as far as possible. In another study, Sarafraz et al.[18] enhanced the conversion factor in a methanol reformer, and for this purpose, they used a

porous catalyst. Moreover, Selimefendigil et al.[19] installed fins that were made of porous media on the back surface of a photovoltaic solar panel and developed artificial neural network models to predict the performance of that. Astanina et al.[20] also considered a porous material as a heat sink to absorb the dissipated heat in the electronic devices and studied that.

In another group of studies, which has a much bigger share in the literature, providing a numerical or analytical solution for a problem has been fulfilled as the main objective. As an example, Chamkha et al.[21] considered a rotating cylinder and solved the mixed convection problem for that, which consisted of the fluid and porous medium as the upper and lower halves, respectively. In addition, Mahmoudi and Karimi[22] investigated a pipe a part that was partially full of porous media numerically in the condition in which there was no thermal equilibrium. Additionally, as a complementary work, the impact of thermal boundary condition was studied in Mahmoudi et al.,[23] while in the references Mahmoudi,[24, 25] the problem under a non-changed heat flux boundary condition and the impact of changes in thermal radiation on its solution were investigated, respectively.

Furthermore, Hooman et al.[26] presented an analytical model to estimate the permeability of gas in a porous media, and Ji et al.[27] also studied the transportation of Hg in a microporous material using simulations. Moreover, Maleki et al.[28] conducted a study for a porous plate in which modeling was done numerically to describe the fluid flow and heat transfer criteria. More investigations were done by their research team in Maleki et al.[29, 30] In the first study,[29] the transport phenomena for nano-fluids were analyzed, while in the second survey,[30] the problem was solved by taking slip and radiation boundary conditions.

In the study of Selimefendigil et al.,[31] by using the superposition, the mixed convection on a porous layer was mathematically solved for a square cavity in a cylinder that rotates. Faraz et al.[32] also carried out their study with the object of finding the solution for the porous slider problem. They used a method called integral transform in the condition of no velocity slip. Another investigation in this field was the one performed by Selimefendigil and Öztop[33] where the performance characteristics of a partly layered porous media were studied by employing the numerical simulation. Selimefendigil and Öztop[33] provided modeling of a U-shaped cavity with a porous part and investigated the impacts of wall corrugation, as well in Selimefendigil and Öztop.[34]

Sheikholeslami[35] proposed a novel computational method to investigate the entropy generation and exergy behavior of nano-fluid in a porous media when there is Lorentz force. One other computer code was also developed by Sheikholeslami[36] to obtain transport phenomena in the problem of flowing a nano-fluid in a porous medium. Additionally, the improvement potential of using porous media in a pipe was evaluated in the study of Mahmoudi and Maerefat.[37] Moreover, in the investigations carried out by Arasteh et al.,[38] Gholamalizadeh et al.,[39] Selimefendigil and Chamkha,[40] Chamkha and Selimefendigil,[41] Keyhani Asl et al.,[42] Zehforoosh et al.,[43] Khashi'ie et al.,[44] Astanina,[45] and Maerefat et al.,[46] either numerical or analytical solutions for employing heat pipe in some other problems have been proposed.

As a member of the second mentioned group of the studies about porous media, here, the Newtonian boundary layer on a porous flat plate is investigated. As the novelty, the governing equations, including the equations for continuity, momentum, and energy, which are from nonlinear partial differential type, are solved using a method, which have both more accuracy and speed of calculation. In the employed method, taking advantage of a similarity

variable, the nonlinear governing equations become ordinary, and then, the analytical solution for them is found by applying the homotopy perturbation method (HPM).[47-49] The HPM has been widely employed as a robust tool for solving similar problems in the studies like Sadeghy et al.,[50] Hayat et al.,[51] Hayat and Abbas,[52] Mamaloukas et al.,[53] Anwar and Makinde,[54] Sajid et al.,[55] Abel et al.,[56] Karimiasl et al.,[57] Jafarimoghaddam,[58] Eldabe and Eldabe,[59] Saradhadevi and Beulah, and [60] and Riaz et al.[61] However, to the best of authors' knowledge, it has not been utilized to solve the problem of this study yet. The methods have also been developed in different studies, such as Yu et al.,[62] Shqair,[63] Altaie et al.,[64] Kharrat and Toma,[65] and De la Luz Sosa et al.[66]

Having provided explanations for this part, that is, Section 1, the details for modeling are presented in Section 2. Then, the results and discussion are given in Section 3, and finally, the conclusions are introduced in Section 4.

2 MODELING

This part provides the details of done modeling, including the generation description and assumptions, governing equations, converting equations to ordinary differential forms, and more details about the equations of the investigated case. They are presented in Sections 2.1–2.5, 2.1–2.5, respectively.

2.1 General description and assumptions

The governing equations for the flow of the boundary layer are solved analytically, and the velocity distribution and temperature distribution are obtained. For this purpose, first, the boundary layer equations, which are in the form of partial derivatives, are converted by similarity transformation to ordinary nonlinear differential equations. In the governing equations, ϑ and u are dependent, and x, y are independent variables. Moreover, T_w is the plate temperature, and $U = U_\infty$ is the free flow rate.

Furthermore, modeling is done by considering the following assumptions:

- The medium is continuous.
- The fluid is incompressible.
- Properties are constant.
- The fluid flow is laminar and steady.
- The flow is single phase.

2.2 HPM

HPM was initially proposed by Ji-Huan He[47] in 1999, and it has been widely used since then because it enjoys the great benefits such as high efficiency in solving nonlinear and even linear problems. HPM method works based on the given description[47]:

Initially, a differential equation, like Equation (1) is assumed, for which the boundary conditions are like Equation (2)[47]:

$$A(u) - f(r) = 0, \quad r \in \Omega \tag{1}$$

$$B\left(u, \frac{\partial u}{\partial n}\right) = 0, \quad r \in \Gamma \tag{2}$$

In Equations (1) and (2), the boundary and general differential operators are shown by A and B, respectively. Moreover, $f(r)$ and Γ denote the analytic function and boundary in Ω space.

There are two parts that make A: one is the linear and another is nonlinear components. Consequently, Equation (1) can be written in the form of Equation (3)[47]:

$$L(u)+N(u)-f(r)=0, \quad r \in \Omega \tag{3}$$

If the homotopy approach[67, 68] is applied, a homotopy structure like $\upsilon(r,p) : \Omega \times [0,1] \rightarrow \mathbb{R}$ could be built in a way that[47]

$$\mathrm{H}(\upsilon, p)=(1-p)[L(\upsilon)-L(u_0)]+p[A(\upsilon)-f(r)]=0, \qquad p \in [0,1], \quad r \in \Omega \tag{4}$$

In another form, Equation (4) could also be expressed as follows[47]:

$$\mathrm{H}(\upsilon, p)= L(\upsilon)-L(u_0)+pL(u_0)+p[N(\upsilon)-f(r)]=0 \tag{5}$$

p, which has a value between 0 and unity, is called the embedding criterion. The initial guess is also shown by u_0. Using Equation (4), Equations (6) and (7) could be obtained[47]:

$$\mathrm{H}(\upsilon, 0)= L(\upsilon)-L(u_0)=0 \tag{6}$$

$$\mathrm{H}(\upsilon, 1)= A(\upsilon)-f(r)=0. \tag{7}$$

Variation of p from 0 to 1 is in a way that of $\mathrm{H}(\upsilon, p)$ from one bound to another one. The bounds are $u_0(r)$ and $u(r)$. The term deformation refers to that. The word "homotopic" also refers to the differences in Equations (6) and (7).

The parameter p is the imbedding criterion. p is small, and it could be stated in the form of power series[47]:

$$\upsilon = \upsilon_0 + p\upsilon_1 + p^2\upsilon_2 + \ldots \tag{8}$$

An approximate answer for Equation (1) is obtained when $p = 1$[47]:

$$u = \lim_{p \to 1} v = v_0 + v_1 + v_2 + \ldots, \tag{9}$$

As the name suggest, HPM is the combination of homotopy approach and perturbation technique. Converging HPM has a direct relation relationship with A, while $N''(\upsilon)$ should be smaller than υ. In addition, having a value of lower than unity for the norm $\frac{L^{-1}\partial N}{\partial \upsilon}$ is necessary for converging the method for a problem. In addition to the original reference, that is, He,[47] more information about HPM could be also found in different studies of He et al., including the recent ones, for example, He and El-Dib[48] and He et al.[49]

2.3 Governing equations

The boundary layer equations are obtained from three main equations: the continuity and the momentum and the energy equations.[69-71] Because the properties are considered constant, the momentum equation is investigated independently from the energy equation.[72] For a two-dimensional laminar and steady flow in a porous medium, the continuity and momentum equations are written as follows:

$$\frac{\partial u}{\partial x} + \frac{\partial \vartheta}{\partial y} = 0 \tag{10}$$

$$\rho\left(u\frac{\partial u}{\partial x} + \vartheta\frac{\partial u}{\partial y}\right) = -\frac{\partial p}{\partial x} + \frac{\partial \tau_{xx}}{\partial x} + \frac{\partial \tau_{xy}}{\partial y} + dF_V \tag{11}$$

$$\rho\left(u\frac{\partial v}{\partial x} + \vartheta\frac{\partial v}{\partial y}\right) = -\frac{\partial p}{\partial y} + \frac{\partial \tau_{yx}}{\partial x} + \frac{\partial \tau_{yy}}{\partial y} + dF_V \tag{12}$$

ρ is the fluid viscosity and the terms $\frac{\partial \tau_{yy}}{\partial y}$ and $\frac{\partial \tau_{xx}}{\partial x}$ are the elastic terms. Additionally, the terms ∂ $\frac{\partial \tau_{yx}}{\partial y}$ and $\frac{\partial \tau_{xy}}{\partial x}$ are viscosity terms dF_v is also the volumetric force.

Based on the boundary layer theory and using the order of magnitude approach,

$$u = \mathrm{O}(1) \qquad \vartheta = \mathrm{O}(\delta) \qquad x = \mathrm{O}(1) \qquad y = \mathrm{O}(\delta) \qquad \frac{\tau_{xx}}{\rho} = \mathrm{O}(1)\frac{\tau_{xy}}{\rho} = \mathrm{O}(\delta)\frac{\tau_{yy}}{\rho} = \mathrm{O}\left(\delta^2\right) \tag{13}$$

By simplifying Equations (11) and (12), Equations (14) and (15) are obtained:

$$\rho\left(u\frac{\partial u}{\partial x} + \vartheta\frac{\partial u}{\partial y}\right) = -\frac{dp}{dx} + \frac{\partial \tau_{xx}}{\partial x} + \frac{\partial \tau_{xy}}{\partial y} - \frac{\mu}{k}u \tag{14}$$

$$\frac{\partial \mathrm{p}}{\partial \mathrm{y}} = 0 \tag{15}$$

$\frac{\mu}{k}u$ is the Darcy term for the porous medium and k is the penetration coefficient. If there was not a porous medium, the pressure gradient in the *x* direction could be ignored. However, because in the investigated problem there is a porous medium, the extended Darcy generalized model could be employed for the outside boundary layer. Therefore,

$$\rho\left(u\frac{\partial u}{\partial x} + \vartheta\frac{\partial u}{\partial y}\right) = -\frac{dp}{dx} + \frac{\partial \tau_{xx}}{\partial x} + \frac{\partial \tau_{xy}}{\partial y} - \frac{\mu}{k}u \tag{16}$$

$$\frac{\partial u}{\partial x} + \frac{\partial \vartheta}{\partial y} = 0 \tag{17}$$

There are five known parameters in Equations (16) and (17), which are p, τ_{xy},τ_{xx}, ϑ, and u.

In order to make number of equations equal to the unknown parameters, and consequently, solve the system of equations, we first need an equation that associates the stress with the deformation field. In the rest of this part, for providing a better insight, the general forms for the equations are written, and finally, they are simplified for the Newtonian fluid.

In general, Equation (18) can be written:

$$\tau_{ij} + \lambda \frac{\Delta}{\Delta t} \tau_{ij} = 2\eta d_{ij} \tag{18}$$

where η is the the coefficient of viscosity and λ is the relaxation time. Furthermore, the time derivative of $\frac{\Delta}{\Delta t}$ is determined from Equation (19):

$$\frac{\Delta \tau_{ij}}{\Delta t} = \frac{D\tau_{ij}}{Dt} - L_{jk}\tau_{ik} - L_{ik}\tau_{kj} \tag{19}$$

in which L_{ij} is the velosity gradient tensor.

By substituting the tension components in Equation (16), the momentum equation is obtained.

$$u\frac{\partial u}{\partial x} + \vartheta \frac{\partial u}{\partial y} + \lambda \left[u^2 \left(\frac{\partial^2 u}{\partial x^2} \right) + \vartheta^2 \left(\frac{\partial^2 u}{\partial y^2} \right) + 2u\vartheta \left(\frac{\partial^2 u}{\partial x \partial y} \right) \right] = -\frac{dp}{dx} + \nu \left(\frac{\partial^2 u}{\partial y^2} \right) - \frac{\nu}{k} u \tag{20}$$

Additionally, according to the generalized Darcy model for porous media,

$$\rho_f \left[\frac{\partial V}{\partial t} + (V.\nabla)V \right] = -\nabla P - \frac{\mu}{K} v \tag{21}$$

$$\rho_f \left[\frac{\partial U}{\partial t} + u\frac{\partial U}{\partial x} + \vartheta \frac{\partial U}{\partial y} \right] = -\frac{dp}{dx} - \frac{\mu}{K} U \tag{22}$$

In addition,

$$\frac{dp}{dx} = -\frac{\mu}{K} U \tag{23}$$

Therefore, it is concluded that

$$u\frac{\partial u}{\partial x} + \vartheta \frac{\partial u}{\partial y} + \lambda \left[u^2 \left(\frac{\partial^2 u}{\partial x^2} \right) + \vartheta^2 \left(\frac{\partial^2 u}{\partial y^2} \right) + 2u\vartheta \left(\frac{\partial^2 u}{\partial x \partial y} \right) \right] = \nu \left(\frac{\partial^2 u}{\partial y^2} \right) - \frac{\nu}{k}(u - U) \tag{24}$$

When there is no slip, the boundary conditions are

$$\text{at} \quad y = 0; \qquad u = 0; \quad \vartheta = 0 \quad \text{at} \quad y \to \infty; \qquad u \to U \tag{25}$$

The general form of the energy equation for a fluid flow on a porous medium is

$$(\rho c)_m \frac{\partial T}{\partial t} + \left(\rho c_p\right)_f V.\nabla T = \nabla.(k_m \nabla T) + \dddot{q}_m \tag{26}$$

In equation (26) $(\rho c)_m$, k_m, and $\dddot{q}_m$ are total thermal capacity, total thermal conductivity coefficient, and total heat production per volume unit of the porous medium, respectively. Because there is no temperature gradient with respect to time (because of the steady-state assumption) and the internal heat generation is 0, the energy equation for the boundary layer could be written in the form of Equations (27) and (28):

$$u\frac{\partial T}{\partial x}+\vartheta\frac{\partial T}{\partial y}=\frac{k_m}{\left(\rho c_p\right)_f}\left(\frac{\partial^2 T}{\partial y^2}\right) \tag{27}$$

$$k_m=(1-\varphi)k_s+\varphi k_f \tag{28}$$

Here, k_s is the solid particle conductivity coefficient and k_f is the fluid conductivity coefficient. The boundary conditions for the energy equation, as shown in Equation (29)

$$\text{at}\quad y=0;\quad T=T_w \qquad \text{at}\quad y\to\infty;\quad T\to T_\infty \tag{29}$$

2.4 Converting equations to ordinary differential forms

By defining the stream function, the number of unknown parameters in Equation (24) is reduced to one:

$$u=\frac{\partial\psi}{\partial y}\qquad \vartheta=-\frac{\partial\psi}{\partial x} \tag{30}$$

By putting Equation (30) in Equation (24), Equation (31) is obtained. (It is done using Maple14 software program.)

$$\left(\frac{\partial\psi}{\partial y}\right)\left(\frac{\partial^2\psi}{\partial x\partial y}\right)-\left(\frac{\partial\psi}{\partial x}\right)\left(\frac{\partial^2\psi}{\partial y^2}\right)+\lambda\left[\left(\frac{\partial\psi}{\partial y}\right)^2,\left(\frac{\partial^3\psi}{\partial y\partial x^2}\right),+,\left(\frac{\partial\psi}{\partial x}\right)^2,\left(\frac{\partial^3\psi}{\partial y^3}\right),\right.$$
$$\left.-,2,\left(\frac{\partial\psi}{\partial y}\right),\left(\frac{\partial\psi}{\partial x}\right),\left(\frac{\partial^3\psi}{\partial x\partial y^2}\right)\right]=\nu\left(\frac{\partial^3\psi}{\partial y^3}\right)-\frac{\nu}{k}\left(\frac{\partial\psi}{\partial y}-U\right) \tag{31}$$

By defining $\eta=y\sqrt{\frac{U}{\nu x}}$:

$$\frac{u}{U}=f'(\eta)\Rightarrow U\,f'(\eta)=\frac{\partial\psi}{\partial y}\ \Rightarrow U\,f'(\eta)=\frac{\partial\psi}{\partial\eta}\frac{\partial\eta}{\partial y}\ \Rightarrow\ Uf'(\eta)=\sqrt{\frac{U}{\vartheta x}}\frac{\partial\psi}{\partial\eta}\ \Rightarrow\sqrt{U\,\vartheta x}\,f'(\eta)d\eta=d\,\psi$$
$$\Rightarrow\psi=\sqrt{U\,\vartheta x}\ f(\eta)$$
(32)

As a result,

$$-2U^2\,kx\ \ f''(\eta)f(\eta)+U^3k\lambda\,\eta\ \ f'^2(\eta)f''(\eta)+U^3k\lambda\ \ f'''(\eta)f^2(\eta)+2U^3k\lambda\ \ f'(\eta)f(\eta)f''(\eta)-4xU^2k\ .$$
$$'(\eta)+4x^2U\nu\ \ f'(\eta)-4Ux^2\nu=0$$
(33)

By multiplying the equation by $\frac{1}{k}$, Equation (34) is obtained:

$$-2U^2x\ \ f''(\eta)f(\eta)+U^3\lambda\,\eta\ \ f'^2(\eta)f''(\eta)+U^3\lambda\ \ f'''(\eta)f^2(\eta)+2U^3\lambda\ \ f'(\eta)f(\eta)f''(\eta)-4xU^2f'''(\eta)+4\frac{x^2}{k}Uv$$

$$f'(\eta)-4U\frac{x^2}{k}v=0$$

(34)

Darcy number is defined as $Da_x=\frac{k}{x^2}=\frac{k_0}{x}\quad k=k_0x,$ which could be found in Equation (34). If the equation is multiplied by $-14U2x$, Equation (35) is obtained:

$$\frac{1}{2}f''(\eta)f(\eta)-\frac{U\lambda}{4x}\,\eta\ \ f'^2(\eta)f(\eta)-\frac{U\lambda}{4x}f'''(\eta)f^2(\eta)-\frac{U\lambda}{2x}f'(\eta)f(\eta)f''(\eta)+\ f'''(\eta)-\frac{1}{Da_x}\frac{v}{Ux}f'(\eta)+\frac{1}{Da_x}\frac{v}{Ux}=0$$

(35)

As a result,

$$f'''(\eta)+\frac{1}{2}\ f(\eta)f''(\eta)-\frac{\lambda U}{4x}\left(2f(\eta)f'(\eta)f''(\eta)+f^2(\eta)f'''(\eta)+\eta f'^2(\eta)f''(\eta)\right)-\frac{1}{Da_x\,Re_x}(f'(\eta)-1)=0$$

(36)

In Equation (36), $De=\frac{\lambda U}{4x}$ and $k^*=\frac{1}{Da^*Re}$. The boundary conditions for the Equation (37) are

$$''(\eta)+\frac{1}{2}\ f(\eta)f''(\eta)-De\left(2f(\eta)f'(\eta)f''(\eta)+f^2(\eta)f'''(\eta)+\eta f'^2(\eta)f''(\eta)\right)-k^*(f'(\eta)-1)=0$$

(37)

$$\eta=0;\qquad f(\eta)=0\qquad f'(\eta)=0\ \ \eta\to\infty;\qquad f'(\eta)\to 1 \tag{38}$$

The energy equation, that is, Equation (27), is considered again. According to the previous discussions and setting the dimensionless temperature $(\theta=\frac{T-T_\infty}{T_w-T_\infty})$ and based on the simplifications in the Maple software program, Equation (39) is obtained:

$$\theta'(\eta)\sqrt{\frac{U}{vx}}\ \ f(\eta)v^2\rho_fc_{pf}\ x+2k_m\ \theta''(\eta)\sqrt{vxU}=0 \tag{39}$$

By Equation (39) by $\sqrt{\frac{vx}{U}}$, Equation (40) is written:

$$\theta'(\eta)f(\eta)v^2\rho_fc_{pf}\ x+2k_mvx\ \ \theta''(\eta)=0 \tag{40}$$

If Equation (40) is multiplied by $\frac{1}{2k_mvx}$, Equation (41) is obtained:

$$\frac{v\rho_fc_{pf}}{2k_m}\ \theta'(\eta)f(\eta)+\theta''(\eta)=0 \tag{41}$$

$$v=\frac{\mu}{\rho}\ pr=\frac{\mu c_p}{k_m}.$$

Therefore,

$$\theta''(\eta)+\frac{1}{2}\ Pr.\ f(\eta)\theta'(\eta)=0 \tag{42}$$

in which boundary conditions could be written as Equation (43) shows:

$$\eta=0;\quad \theta(\eta)=0\ \ \eta\to\infty;\quad \theta(\eta)\to 1 \tag{43}$$

2.5 The investigated case: Newtonian fluid flow in the porous medium on the flat plate

In order to solve the problem, first, the momentum equation is considered, and by solving it, *f* is determined. Then, by putting *f* into, solving the energy equation is done. For this case, it is enough to consider both *De* and *R* in Equation (36) 0. For this case,

$$f'''(\eta)+\frac{1}{2}\ f(\eta)f''(\eta)-k^*(f'(\eta)-1)=0 \tag{44}$$

$$f(0)=0 \qquad f'^{(0)}=0 \qquad f'(\infty)\to 1 \tag{45}$$

In order to obtain $f(\eta)$, the auxiliary linear operator, introduced in equation (46), is utilized:

$$L(u)=f'''(\eta)+\zeta f''(\eta) \tag{46}$$

The corresponding differential equation could be written as follows:

$$\frac{d^3f}{d\eta^3}+\zeta\frac{d^2f}{d\eta^2}=0 \tag{47}$$

The boundary conditions, in this case, are

$$f(0)=0,\quad f'^{(0)}=0 \qquad f'(\infty)=1 \tag{48}$$

The value of ζ is adjusted in a way that the least possible error compared to the numerical answer is achieved.

By solving the differential equation that has been presented in Equation (47), the corresponding solution to the auxiliary linear operator is obtained with the boundary conditions of the problem. This function, which is also called the guess function, is equal to

$$f^0(\eta)=-\frac{5}{6}+\frac{5}{6}\ \eta+e^{\left(-\frac{6}{5}\eta\right)} \tag{49}$$

In the HPM, the equation and the corresponding boundary conditions for the present problem are expressed as

$$(1-p)L\left[F(\eta;p)-f^0(\eta)\right]+p[L\{F(\eta;p)+N\{F(\eta;p)\}]=0 \tag{50}$$

$$F(0;p)=0,\quad F'(0;p)=0 \qquad F'(\infty;p)=1 \tag{51}$$

where p is called the embedding parameter that is $p \in [0 \text{ ، } 1]$. $L[F(\eta; p)+N(F(\eta; p)]$ refers to the equation. For $p = 0$ and $p = 1$, we have

$$F(\eta; 0)= f_0(\eta) \qquad F(\eta; 1)= f(\eta) \tag{52}$$

Therefore, when P increases from 0 to 1, $F(\eta; p)$ changes from $f_0(\eta)$ to $f(\eta)$. The equation for $k^* = 0.2$ is solved by Maple, which leads to obtaining the following solution:

$$(1-p)\left(f'''(\eta)+1.2\, f''(\eta)-\left(-\frac{5}{6}+\frac{5}{6}\,\eta+e^{\left(-\frac{6}{5}\eta\right)}\right)\right)+p\left(f'''(\eta)+\frac{1}{2}\, f(\eta)f''(\eta)-0.2f'(\eta)+0.2\right)=0$$

(53)

By considering f in the form of $f(\eta) = f_0(\eta)+pf_1(\eta)+p^2f_2(\eta)$ in Equation (53) and sorting it based on p, $f_0(\eta)$, $f_1(\eta)$ and $f_2(\eta)$ are obtained.

$$f_0(\eta)= -0.8333384535 + 1.0000006144\eta + 0.8333384535e^{-1.20000\eta} \tag{54}$$

$$f_1(\eta)= 0.2834793696\, e^{-1.20000\eta} + 0.5138899132e^{-1.20000\eta}\,\eta - 0.2083358934e^{-1.20000\eta}\eta^2 + 0.07233885188\, e^{-2.40000\eta} + 0.0000051200\,\eta^2 - 0.0001014232219\eta - 0.3558182220$$

(55)

$$f_2(\eta)= 0.1454575023e^{-1.20000\eta} - 0.000007655488529\eta^2 + 0.1842524056e^{-1.20000\eta}\,\eta + 0.2612133621e^{-1.20000\eta}\eta^2 + 0.01857138921e^{-2.40000\eta} - 0.00000004266710357\,\eta^3 + 0.02604214668e^{-1.20000\eta}\eta^4 - 0.1284733388e^{-1.20000\eta}\eta^3 + 0.006977169786e^{-3.600000\eta} + 0.05907617355\eta e^{-2.400000\eta} - 0.03616964817e^{-2.4000000\eta}\eta^2 + 0.0009095667116\,\eta - 0.1710060599$$

(56)

Consequently, $f(\eta)$ is determined:

$$f(\eta)= -0.8333384535 + 1.0000006144\eta + 0.8333384535e^{-1.20000\eta} + 0.2834793696\, e^{-1.20000\eta} + 0.5138899132e^{-1.20000\eta}\,\eta - 0.2083358934e^{-1.20000\eta}\eta^2 + 0.07233885188\, e^{-2.40000\eta} + 0.0000051200\,\eta^2 - 0.0001014232219\eta - 0.3558182220 + 0.1454575023e^{-1.20000\eta} - 0.000007655488529\eta^2 + 0.1842524056e^{-1.20000\eta}\,\eta + 0.2612133621e^{-1.20000\eta}\eta^2 + 0.01857138921e^{-2.40000\eta} - 0.00000004266710357\,\eta^3 + 0.02604214668e^{-1.20000\eta}\eta^4 - 0.1284733388e^{-1.20000\eta}\eta^3 + 0.006977169786e^{-3.600000\eta} + 0.05907617355\eta e^{-2.400000\eta} - 0.03616964817e^{-2.4000000\eta}\eta^2 + 0.0009095667116\eta - 0.1710060599$$

(57)

Next, the energy equation is solved. As indicated before, for this purpose, $f(\eta)$is known from the solved momentum equation. Here, the auxiliary linear operator introduced in Equation (58) is considered:

$$L(u)= \theta''(\eta)+\theta'(\eta) \tag{58}$$

The corresponding differential equation is expressed as follows:

$$\frac{d^2\theta}{d\eta^2}+\frac{d\theta}{d\eta}=0 \tag{59}$$

While in this case, the boundary conditions are

$$\theta(0)= 0 \quad \theta(\infty)= 1 \tag{60}$$

Having the similar fashion as the momentum equation, the guess function can be also used here:

$$\theta^0(\eta)= 1 - e^{-\eta} \tag{61}$$

Again, like the momentum equation, Equations (62) and (63) could be written, which leads to finding the analytical solution. Equation (64) presents the obtained solution when Pr = 0.7 and k^* = 0.2, which is determined by Maple software program:

$$(1 - p)L\left[\theta(\eta; p)-\theta^0(\eta)\right]+p[L\{\theta(\eta; p)+N\{\theta(\eta; p)\}]= 0 \tag{62}$$

$$\theta(0; p)= 0 \qquad \theta(\infty; p)= 1 \tag{63}$$

$$(1 - p)\left(\theta''(\eta)+\theta'(\eta)-\left(1 - e^{-\eta}\right)\right)+p\left(\theta''(\eta)+\frac{1}{2}\ 0.7\ f(\eta)\ \theta'(\eta)\right)= 0 \tag{64}$$

If the energy function is considered as θ (η) = θ_0 (η) + $p\theta$_1 (η) + p ^ 2 θ_2 (η), and the similar process is done, $\theta_0(\eta)$, $\theta_1(\eta)$, and $\theta_2(\eta)$ are obtained in the form of Equations (65)–(67), respectively.

$$\theta_0(\eta)= 1.000045402 - 1.000045402e^{-\eta} \tag{65}$$

$$\theta_1(\eta)= 0.005772372713\eta^2 e^{-2.20000\eta} - 0.07598024962\ \eta\ e^{-2.20000\eta} - 0.2695810668\ e^{-2.20000\eta} - 0.003452714078\ \eta^4 e^{-2.20000\eta} - 0.004513271260\ e^{-3.40000\eta} + 0.001551464659\eta^2 e^{-3.40000\eta} - 0.0003285060603\eta\ e^{-3.40000\eta} - 0.0001474710324\ e^{-4.60000\eta} + 0.2745382680e^{-\eta} - 0.00296458 \tag{66}$$

$$\theta_2(\eta)= -0.0000844859547e^{-5.80000\eta} - 0.000001492740922\ e^{-7\eta} - 0.00000002805857037\ e^{-8.20000\eta} - 0.000000000069693480 20\ \eta^8 e^{-\eta} - 0.0009932741947\ \eta\ e^{-4.60000\eta} - 0.00441469983\ \eta^5 e^{-2.20000\eta} + 0.0006047123667\ \eta^6 e^{-2.20000\eta} + 0.0034736092\ \eta^3 e^{-3.40000\eta} - \ldots - 0.01533864715\eta^4 e^{-\eta} \tag{67}$$

As an important point, it is worth mentioning that despite having employed widely, the differential model for the porous medium is an approximate one, and it is not able to model the effect of porosity (size and distribution) on the flow properties. It is taken into account as a limitation of the current work, and using two-scale fractal calculus could be suggested to overcome that for future research.

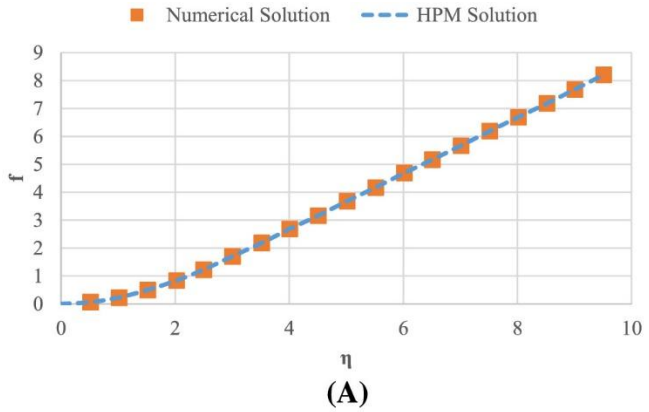

(A)

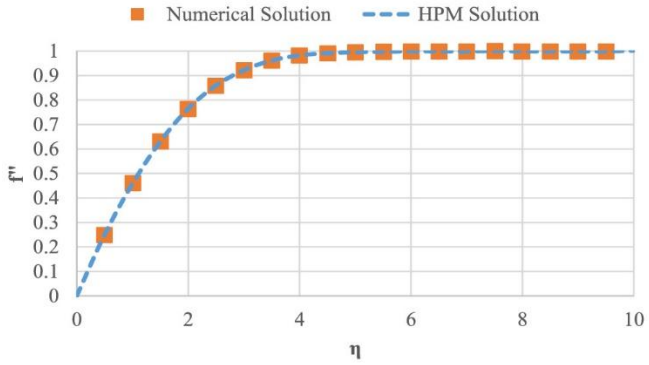

(B)

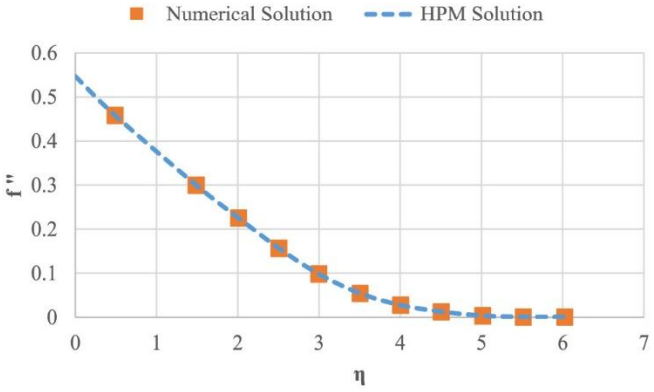

(C)

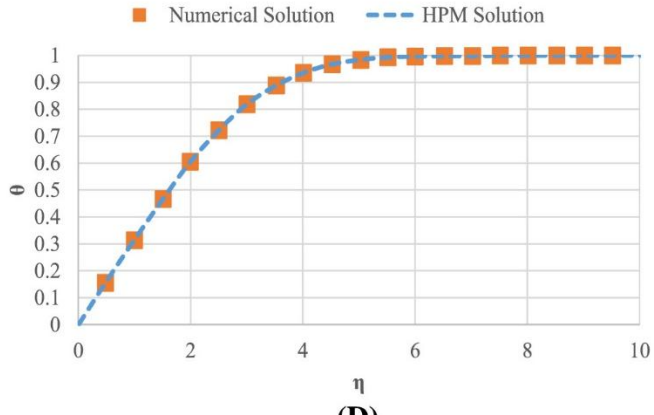

(D)

FIGURE 1.Comparing the accuracy of homotopy perturbation method (HPM) solution with the numerical one for k^* = 0.2,*De* = 0.01 for different parameters (A) stream function, (B) velocity distribution, (C) stress distribution, and (D) dimensionless temperature

3 VALIDATION

As it has been indicated in different studies in various fields of knowledge, including Sohani et al.,[73-77] for each simulation approach, validation is a necessary part to become sure about working the approach in a satisfactory way. Therefore, validation is done. For this purpose, the prediction of the HPM for different cases is compared with the numerical method of boundary value problems calculated by the Maple software. The comparison is done using the profiles for the dimensionless stream function, velocity distribution, stress distribution, and heat distribution, which are all illustrated in Figure 1A–D, respectively. Figure 1 has provided an acceptable accuracy, which confirms that the developed analytical model is valid. In addition, as observed, when η goes up, the function f has an almost linear enhancement, while the function f' increases and approaches a constant value. The behavior of θ function is the same as f', whereas the function f'' experiences a drastic decrease and approaching a constant level afterward.

4 CONCLUSION

In this study, the HPM was employed to provide an analytical solution for a given problem, which was flowing a Newtonian fluid on a flat porous plate. The problem was defined by presenting the governing equations as well as the boundary conditions, and then, the working principle of HPM was introduced. Next, the momentum and energy equations are solved using the HPM. Finally, the obtained analytical solution was validated using the profiles for four important indicators related to the problem, which were stream function, velocity and stress distribution, and dimensionless temperature profiles. The results implied that there was a perfect agreement between the analytical and numerical solutions, based on which the developed analytical solution was verified. Moreover, as the validation data showed, increasing η leads to increase in f' and θ functions initially, and they got constant then. Furthermore, f' had a downward trend and approached a constant value. The function f also went up almost linearly.

ACKNOWLEDGEMENT

There are no funders to report for this submission.

CONFLICT OF INTERESTS

This work does not have any conflict of interests.

REFERENCES

1. Zhao C, Opolot M, Liu M, Bruno F, Mancin S, Hooman K. Numerical study of melting performance enhancement for PCM in an annular enclosure with internal-external fins and metal foams. *Int J Heat Mass Transf*. 2020; 150: 119348.

2. Dong P, Li X, Sun Y, et al. Numerical investigation of the influence of local effects on the transient start-up process of natural draft dry cooling towers in dispatchable power plants. *Int J Heat Mass Transf*. 2019; 133: 166- 178.

3. Habib R, Yadollahi B, Karimi N, Doranegard MH. On the unsteady forced convection in porous media subject to inlet flow disturbances—a pore-scale analysis. *Int Commun Heat Mass Transf*. 2020; 116: 104639.

4. Sheikholeslami M, Arabkoohsar A, Ismail KAR. Entropy analysis for a nanofluid within a porous media with magnetic force impact using non-Darcy model. *Int Commun Heat Mass Transf*. 2020; 112: 104488.

5. Dong P, Li X, Hooman K, et al. The crosswind effects on the start-up process of natural draft dry cooling towers in dispatchable power plants. *Int J Heat Mass Transf*. 2019; 135: 950- 961.

6. Dai Y, Kaiser AS, Lu Y, Klimenko AY, Dong P, Hooman K. Addressing the adverse cold air inflow effects for a short natural draft dry cooling tower through swirl generation. *Int J Heat Mass Transf*. 2019; 145: 118738.

7. Chakkingal M, de Geus J, Kenjereš S, Ataei-Dadavi I, Tummers MJ, Kleijn CR. Assisting and opposing mixed convection with conjugate heat transfer in a differentially heated cavity filled with coarse-grained porous media. *Int Commun Heat Mass Transf*. 2020; 111: 104457.

8. Nikan O, Machado JAT, Golbabai A, Nikazad T. Numerical approach for modeling fractal mobile/immobile transport model in porous and fractured media. *Int Commun Heat Mass Transf*. 2020; 111: 104443.

9. Wu H, Fang C, Wu R, Qiao R. Drying of porous media by concurrent drainage and evaporation: a pore network modeling study. *Int J Heat Mass Transf*. 2020; 152: 118718.

10. Feng X-B, Liu Q, He Y-L. Numerical simulations of convection heat transfer in porous media using a cascaded lattice Boltzmann method. *Int J Heat Mass Transf*. 2020; 151: 119410.

11. Haq RU, Raza A, Algehyne EA, Tlili I. Dual nature study of convective heat transfer of nanofluid flow over a shrinking surface in a porous medium. *Int Commun Heat Mass Transf*. 2020; 114: 104583.

12. Krishna MV, Chamkha AJ. Hall and ion slip effects on MHD rotating flow of elastico-viscous fluid through porous medium. *Int Commun Heat Mass Transf*. 2020; 113: 104494.

13. Habib R, Karimi N, Yadollahi B, Doranehgard MH, Li LKB. A pore-scale assessment of the dynamic response of forced convection in porous media to inlet flow modulations. *Int J Heat Mass Transf*. 2020; 153: 119657.

14. Izadi M, Sheremet MA, Mehryan SAM, Pop I, Öztop HF, Abu-Hamdeh N. MHD thermogravitational convection and thermal radiation of a micropolar nanoliquid in a porous chamber. *Int Commun Heat Mass Transf*. 2020; 110: 104409.

15. Sheikholeslami M, Shah Z, Shafee A, Kumam P, Babazadeh H. Lorentz force impact on hybrid nanofluid within a porous tank including entropy generation. *Int Commun Heat Mass Transf*. 2020; 116: 104635.

16. Kholghi SA, Hanafizadeh P, Karbalaee S, Ashjaee M. Analysis of air flow and heat transfer in a winding using porous medium approach. *Int Commun Heat Mass Trans*. 2020; 112:104485.

17. Sheikholeslami M, Jafaryar M, Shafee A, Babazadeh H. Acceleration of discharge process of clean energy storage unit with insertion of porous foam considering nanoparticle enhanced paraffin. *J Clean Prod*. 2020; 261: 121206.

18. Sheikholeslami M, Jafaryar M, Abohamzeh E, Shafee A, Babazadeh H. Energy and entropy evaluation and two-phase simulation of nanoparticles within a solar unit with impose of new turbulator. *Sustain. Energy Technol. Assess*. 2020; 39: 100727.

19. Selimefendigil F, Bayrak F, Oztop HF. Experimental analysis and dynamic modeling of a photovoltaic module with porous fins. *Renew Energy*. 2018; 125: 193- 205.

20. Astanina MS, Rashidi MM, Sheremet MA, Lorenzini G. Cooling system with porous finned heat sink for heat-generating element. *Transport Porous Med*. 2020; 133: 1- 20.

21. Chamkha AJ, Selimefendigil F, Ismael MA. Mixed convection in a partially layered porous cavity with an inner rotating cylinder. *Numer Heat Transf Part A: Appl*. 2016; 69(6): 659- 675.

22. Mahmoudi Y, Karimi N. Numerical investigation of heat transfer enhancement in a pipe partially filled with a porous material under local thermal non-equilibrium condition. *Int J Heat Mass Transf*. 2014; 68: 161- 173.

23. Mahmoudi Y, Karimi N, Mazaheri K. Analytical investigation of heat transfer enhancement in a channel partially filled with a porous material under local thermal non-equilibrium condition: effects of different thermal boundary conditions at the porous-fluid interface. *Int J Heat Mass Transf*. 2014; 70: 875- 891.

24. Mahmoudi Y. Constant wall heat flux boundary condition in micro-channels filled with a porous medium with internal heat generation under local thermal non-equilibrium condition. *Int J Heat Mass Transf*. 2015; 85: 524- 542.

25. Mahmoudi Y. Effect of thermal radiation on temperature differential in a porous medium under local thermal non-equilibrium condition. *Int J Heat Mass Transf*. 2014; 76: 105- 121.

26. Hooman K, Tamayol A, Dahari M, Safaei MR, Togun H, Sadri R. A theoretical model to predict gas permeability for slip flow through a porous medium. *Appl Therm Eng*. 2014; 70(1): 71- 76.

27. Ji G, George A, Skoulou V, et al. Investigation and simulation of the transport of gas containing mercury in microporous silica membranes. *Chem Eng Sci*. 2018; 190: 286- 296.

28. Maleki H, Safaei MR, Togun H, Dahari M. Heat transfer and fluid flow of pseudo-plastic nanofluid over a moving permeable plate with viscous dissipation and heat absorption/generation. *J Therm Anal Calorim*. 2019; 135(3): 1643- 1654.

29. Maleki H, Safaei MR, Alrashed AAAA, Kasaeian A. Flow and heat transfer in non-Newtonian nanofluids over porous surfaces. *J Therm Anal Calorim*. 2019; 135(3): 1655- 1666.

30. Maleki H, Alsarraf J, Moghanizadeh A, Hajabdollahi H, Safaei MR. Heat transfer and nanofluid flow over a porous plate with radiation and slip boundary conditions. *J Cent South Univ*. 2019; 26(5): 1099- 1115.

31. Selimefendigil F, Ismael MA, Chamkha AJ. Mixed convection in superposed nanofluid and porous layers in square enclosure with inner rotating cylinder. *Int J Mech Sci*. 2017; 124: 95- 108.

32. Faraz N, Khan Y, Lu DC, Goodarzi M. Integral transform method to solve the problem of porous slider without velocity slip. *Symmetry*. 2019; 11(6): 791.

33. Selimefendigil F, Öztop HF. Effects of local curvature and magnetic field on forced convection in a layered partly porous channel with area expansion. *Int J Mech Sci*. 2020; 179: 105696.

34. Selimefendigil F, Öztop HF. Magnetohydrodynamics forced convection of nanofluid in multi-layered U-shaped vented cavity with a porous region considering wall corrugation effects. *Int Commun Heat Mass Transf*. 2020; 113: 104551.

35. Sheikholeslami M. New computational approach for exergy and entropy analysis of nanofluid under the impact of Lorentz force through a porous media. *Comput Methods Appl Mech Eng*. 2019; 344: 319- 333.

36. Sheikholeslami M. Numerical approach for MHD Al2O3-water nanofluid transportation inside a permeable medium using innovative computer method. *Comput Methods Appl Mech Eng*. 2019; 344: 306- 318.

37. Mahmoudi Y, Maerefat M. Analytical investigation of heat transfer enhancement in a channel partially filled with a porous material under local thermal non-equilibrium condition. *Int J Therm Sci*. 2011; 50(12): 2386- 2401.

38. Arasteh H, Mashayekhi R, Goodarzi M, Motaharpour SH, Dahari M, Toghraie D. Calorimetry, heat and fluid flow analysis of metal foam embedded in a double-layered sinusoidal heat sink under local thermal non-equilibrium condition using nanofluid. *J Therm Anal Calorim*. 2019; 138(2): 1461- 1476.

39. Gholamalizadeh E, Pahlevanzadeh F, Ghani K, Karimipour A, Nguyen TK, Safaei MR. Simulation of water/FMWCNT nanofluid forced convection in a microchannel filled with porous material under slip velocity and temperature jump boundary conditions. *Intl J Numer Method Heat Fluid Flow*. 2019; 30(5): 2329- 2349.

40. Selimefendigil F, Chamkha AJ. MHD mixed convection of Ag–MgO/water nanofluid in a triangular shape partitioned lid-driven square cavity involving a porous compound. *J Therm Anal Calorim*. 2020; 2: 1- 18.

41. Chamkha AJ, Selimefendigil F. MHD free convection and entropy generation in a corrugated cavity filled with a porous medium saturated with nanofluids. *Entropy*. 2018; 20(11): 846.

42. Keyhani Asl A, Hossainpour S, Rashidi MM, Sheremet MA, Yang Z. Comprehensive investigation of solid and porous fins influence on natural convection in an inclined rectangular enclosure. *Int J Heat Mass Transf*. 2019; 133: 729- 744.

43. Zehforoosh A, Hossainpour S, Rashidi MM. Heat generating porous matrix effects on Brownian motion of nanofluid. *Intl J Numer Method Heat Fluid Flow*. 2019; 29(5): 1724-1740.

44. Khashi'ie NS, Arifin NM, Rashidi MM, Hafidzuddin EH, Wahi N. Magnetohydrodynamics (MHD) stagnation point flow past a shrinking/stretching surface with double stratification effect in a porous medium. *J Therm Anal Calorim*. 2019; 139: 1-14.

45. Astanina MS, Rashidi MM, Sheremet MA, Lorenzini G. Effect of porous insertion on convective energy transport in a chamber filled with a temperature-dependent viscosity liquid in the presence of a heat source term. *Int J Heat Mass Transf*. 2019; 144: 118530.

46. Maerefat M, Mahmoudi SY, Mazaheri K. Numerical simulation of forced convection enhancement in a pipe by porous inserts. *Heat Transf Eng*. 2011; 32(1): 45- 56.

47. He J-H. Homotopy perturbation technique. *Comput Methods Appl Mech Eng*. 1999; 178(3): 257- 262.

48. He J-H, El-Dib YO. Homotopy perturbation method for Fangzhu oscillator. *J Math Chem*. 2020; 58(10): 2245- 2253.

49. He JH, El-Dib YO. The reducing rank method to solve third-order Duffing equation with the homotopy perturbation. *Numer. Methods Partial Differ. Equ.* 2020. https://doi.org/10.1002/num.22609

50. Sadeghy K, Najafi A-H, Saffaripour M. Sakiadis flow of an upper-convected Maxwell fluid. *Int J Non-Linear Mech*. 2005; 40(9): 1220- 1228.

51. Hayat T, Abbas Z, Sajid M. Series solution for the upper-convected Maxwell fluid over a porous stretching plate. *Phys Lett A*. 2006; 358(5): 396- 403.

52. Hayat T, Abbas Z. Heat transfer analysis on the MHD flow of a second grade fluid in a channel with porous medium. *Chaos Soliton Fract*. 2008; 38(2): 556- 567.

53. .Mamaloukas C, Abel MS, Tawade JV, Mahabaleswar US. On effects of a transverce magnetic field on an UCM fluid over a stretching sheet. *Int J Pure Appl Math*. 2011; 661: 1-9.

54. Bég OA, Makinde OD. Viscoelastic flow and species transfer in a Darcian high-permeability channel. *J Petrol Sci Eng*. 2011; 76(3): 93- 99.

55. Sajid M, Iqbal Z, Hayat T, Obaidat S. Series solution for rotating flow of an upper convected Maxwell fluid over a stretching sheet. *Commun Theor Phys*. 2011; 56(4): 740- 744.

56. Abel MS, Tawade JV, Shinde JN. The effects of MHD flow and heat transfer for the UCM fluid over a stretching surface in presence of thermal radiation. *Adv Math Phys*. 2012; 2012:702681. https://doi.org/10.1155/2012/702681

57. Karimiasl M, Ebrahimi F, Mahesh V. Postbuckling analysis of piezoelectric multiscale sandwich composite doubly curved porous shallow shells via Homotopy perturbation method. *Eng Comput*. 2019; 37: 1- 17.

58. Jafarimoghaddam A. Two-phase modeling of three-dimensional MHD porous flow of upper-convected Maxwell (UCM) nanofluids due to a bidirectional stretching surface: Homotopy perturbation method and highly nonlinear system of coupled equations. *Eng Sci Technol an Int J*. 2018; 21(4): 714- 726.

59. Eldabe NT, Abou-zeid MY. Homotopy perturbation method for MHD pulsatile non-Newtonian nanofluid flow with heat transfer through a non-Darcy porous medium. *J Egypt Math Soc*. 2017; 25(4): 375- 381.

60. Saradhadevi T, Beulah RD. Distribution of temperature on a porous fin exposed to uniform magnetic field to a vertical isothermal surface by homotopy perturbation method. Journal of Seybold Report ISSN NO 1533 9211.

61. Riaz A, Zeeshan A, Bhatti MM, Ellahi R. Peristaltic propulsion of Jeffrey nano-liquid and heat transfer through a symmetrical duct with moving walls in a porous medium. *Physica A Stat Mech Appl*. 2020; 545: 123788.

62. Yu D-N, He J-H, Garcıa AG. Homotopy perturbation method with an auxiliary parameter for nonlinear oscillators. *J Low Freq Noise V A*. 2019; 38(3–4): 1540- 1554.

63. Shqair M. Developing a new approaching technique of homotopy perturbation method to solve two-group reflected cylindrical reactor. *Results Phys*. 2019; 12: 1880- 1887.

64. Altaie SA, Jameel AF, Saaban A. Homotopy perturbation method approximate analytical solution of fuzzy partial differential equation. *IAENG Int J Appl Math*. 2019; 49(1): 22- 28.

65. Kharrat BN, Toma GA. Development of homotopy perturbation method for solving nonlinear algebraic equations. *Int J Sci Res MathStat Sci*. 2020; 7(2): 47- 50.

66. De la Luz Sosa J, Olvera-Trejo D, Urbikain G, Martinez-Romero O, Elías-Zúñiga A, Lacalle LN. Uncharted stable peninsula for multivariable milling tools by high-order homotopy perturbation method. *Appl Sci*. 2020; 10(21):7869. https://doi.org/10.3390/app10217869

67. Liao S-J. An approximate solution technique not depending on small parameters: a special example. *Int J Non-Linear Mech*. 1995; 30(3): 371- 380.

68. Liao S-J. Boundary element method for general nonlinear differential operators. *Eng Anal Bound Elem*. 1997; 20(2): 91- 99.

69. Sarafraz MM, Safaei MR, Goodarzi M, Arjomandi M. Reforming of methanol with steam in a micro-reactor with Cu–SiO_2 porous catalyst. *Int J Hydrogen Energy*. 2019; 44(36): 19628- 19639.

70. Nazari S, Ellahi R, Sarafraz MM, Safaei MR, Asgari A, Akbari OA. Numerical study on mixed convection of a non-Newtonian nanofluid with porous media in a two lid-driven square cavity. *J Therm Anal Calorim*. 2020; 140(3): 1121- 1145.

71. Safaei MR, Safdari Shadloo M, Goodarzi MS, et al. A survey on experimental and numerical studies of convection heat transfer of nanofluids inside closed conduits. *Adv Mech Eng*. 2016; 8(10). https://doi.org/10.1177/1687814016673569

72. Safaei MR, Ahmadi G, Goodarzi MS, Kamyar A, Kazi SN. Boundary layer flow and heat transfer of FMWCNT/water nanofluids over a flat plate. *Fluids*. 2016; 1(4): 31. https://doi.org/10.3390/fluids1040031

73. Sohani A, Sayyaadi H. Providing an accurate method for obtaining the efficiency of a photovoltaic solar module. *Renew Energy*. 2020; 156: 395- 406.

74. Sohani A, Zamani Pedram M, Hoseinzadeh S. Determination of Hildebrand solubility parameter of pure 1-alkanols up to high pressures. *J Mol Liq*. 2020; 297: 111847.

75. Sohani A, Hoseinzadeh S, Berenjkar K. Experimental analysis of innovative designs for solar still desalination technologies; an in-depth technical and economic assessment. *J Energy Storage*. 2021; 33:101862.

76. Sohani A, Shahverdian MH, Sayyaadi H, Garcia DA. Impact of absolute and relative humidity on the performance of mono and poly crystalline silicon photovoltaics; applying artificial neural network. *J Clean Prod*. 2020; 276: 123016.

77. Sohani A, Sayyaadi H. Employing genetic programming to find the best correlation to predict temperature of solar photovoltaic panels. *Energ Conver Manage*. 2020; 224:113291.